Insight into clogging of micromachined cryogenic coolers

Cite as: Appl. Phys. Lett. **90**, 064102 (2007); https://doi.org/10.1063/1.2472194
Submitted: 21 November 2006 . Accepted: 10 January 2007 . Published Online: 07 February 2007

P. P. P. M. Lerou, H. J. M. ter Brake, H. J. Holland, J. F. Burger, and H. Rogalla

Insight into clogging of micromachined cryogenic coolers

P. P. P. M. Lerou,[a] H. J. M. ter Brake,[b] H. J. Holland, J. F. Burger, and H. Rogalla
Low Temperature Division, Faculty of Science and Technology, University of Twente, P.O. Box 217, 7500 AE Enschede, The Netherlands

(Received 21 November 2006; accepted 10 January 2007; published online 7 February 2007)

Cryogenic microcoolers can be used to cool small electronic devices to improve their performance. The authors present a micro-cold-stage of only 0.05 cm^3 that cools to 96 K, applying Joule-Thomson expansion in a 300 nm high flow restriction. Critical in such a microcooler is the deposition of water molecules that migrate to the restriction and block the flow. Because the microcooler is made of glass the authors had the unique opportunity to monitor this phenomenon and combine this visualization with experimental data. This provides significant insight in the way this clogging develops and opens possibilities to realize stable operation. © *2007 American Institute of Physics*. [DOI: 10.1063/1.2472194]

The performance of electronic devices can often be improved by lowering the operating temperature, resulting in lower noise and larger speed.[1] Also, specific phenomena can be applied at low temperatures, for instance, superconductivity.[2] Although these electronic devices are very small ($\ll 1$ cm^3), correspondingly small cryogenic coolers are not yet available. A major hurdle in developing microcoolers is clogging of the small channels because of moisture. In our microcooler project we had the unique opportunity to visualize this clogging mechanism. In this letter, we describe this mechanism and give a strategy to prevent clogging and to secure the operation of a micro-cold-stage.

The experiments were performed on a micro-cold-stage that can cool down to 100 K with a cooling power of 10 mW and measures only $30\times2\times0.5$ mm^3 (≈0.05 cm^3).[3] Cooling is obtained by expanding nitrogen over a flow restriction that is 300 nm high. In contrast to earlier micro-cold-stages,[4,5] this cold tip is optimized for maximum performance in combination with minimal size.[6] Also, the production is fully based on microelectro mechanical system (MEMS) technology which makes it suitable for mass production, integration with integrated circuit technology based circuitry, and microvacuum packaging.[7–9] The microcooler is based on a Joule-Thomson cycle in which nitrogen expands over a flow restriction from 80 to 6 bars. The temperature of the cold tip, 96 K, is determined by the boiling temperature of nitrogen at 6 bars. The high and low pressures determine the available difference in specific enthalpy of the gas (dh). The cooling power (P_{cool}) is determined by the mass flow ($\dot{m}$): $P_{cool}=\dot{m}dh$. This flow is chosen at 1 mg s^{-1} which results in a gross cooling power of about 15 mW. In order to reduce parasitic heat loads to below this level, the cooler has to be operated in a vacuum environment. At the given pressures, the flow rate is determined by the restriction, in our case a very shallow channel of only 300 nm high. Further clarification of the cycle and the chosen parameters can be found in Ref. 6.

The cold stage consists of a stack of three glass wafers.[3] In the top wafer, the high-pressure line is etched as a rectangular channel with supporting pillars. This line ends in a flow restriction and an evaporator volume that crosses the center wafer into the bottom wafer. This bottom wafer contains the low-pressure line, again etched as a rectangular channel containing supporting pillars, thus forming a counterflow heat exchanger (CFHX). A critical issue in the operation of this cooler is clogging caused by the deposition of water molecules. By utilizing the fact that the cooler is built out of glass wafers we had the opportunity to monitor and visualize this clogging phenomenon.

In the measurement setup, high-purity nitrogen gas 6.0 is supplied from a gas bottle and led through a getter stabilized zeolite filter. According to its specifications, the outlet contamination should be below 1 ppb (parts per billion). Therefore, the contamination in the cooler is determined by the amount present at start-up. To minimize this initial contamination in the system, the setup is cleaned by pumping and heating. Through calculation,[10] the initial pressure inside the cold stage was estimated at about 1 Pa. In our experiments, the temperature at which the restriction starts to clog appeared to lie around 200 K. From the relevant fluids, water is the only one that has a phase transition around that temperature at about 1 Pa. The left graph of Fig. 1 shows the phase diagram of water. It can be seen that water changes its phase in the deposition from vapor to solid at about 200 K and 1 Pa.

A typical cooldown registration is depicted in Fig. 2. The experimental mass-flow curve corresponds to theory (i.e., restriction height of 300 nm) for temperatures above 200 K. At around that temperature ($p_{partial,H_2O}=1$ Pa≈0.1 ppm), the mass-flow curve shows a small decrease of the slope. This is an indication that the restriction is getting partly clogged (point A). A layer of a few nanometers on the surface of the restriction already accounts for the measured effect. It results in a decrease of the mass flow and thus of cooling power. Nevertheless, the cooldown continues and below about 120 K, the mass flow starts to fluctuate (point B). This mass-flow fluctuation indicates that liquid is being formed inside the evaporator. It also means that there is a relatively large temperature gradient from the evaporator to the flow restriction since at 6 bars nitrogen boils at 96 K. The liquid nitrogen in the evaporator further cools the restriction, thus affecting the flow as depicted in Fig. 2. In the top graph of this figure, it can be seen that the measured temperature does not

[a]Electronic mail: p.p.p.m.lerou@utwente.nl
[b]Author to whom correspondence should be addressed; FAX: +31-53-489-1099; electronic mail: h.j.m.terbrake@utwente.nl

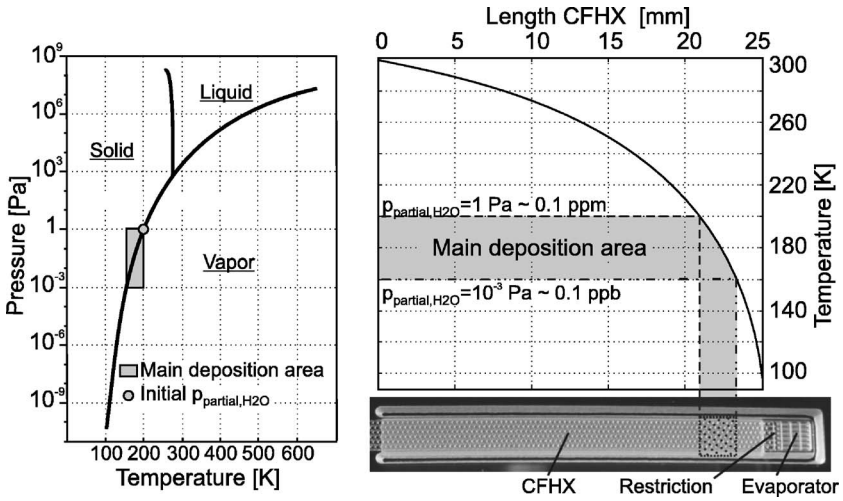

FIG. 1. Left: phase diagram of water. Data above 200 K are taken from Ref. 13. Data below 200 K are calculated using the Clausius-Clapeyron equation. Right: calculated temperature profile of the CFHX (Ref. 6) and a schematic representation of the main deposition area. Right bottom: photograph of a cold stage.

reach the predicted 96 K but is about 110 K. This temperature is measured with a thermocouple connected to the outside of the evaporator. The temperature difference of 14 K is caused by the thermal resistance formed by the thin layer of glass and the connection between the thermocouple and the cold stage.

From point C, the cold tip stays in a semistable situation with constant flow and temperature. In this phase, there is a constant temperature gradient over the CFHX from about 100 K at the cold tip to 300 K at the warm end, see right plot in Fig. 1. The coldest part of the CFHX with a temperature below 200 K now acts as a water filter. Here, water molecules deposit on the CFHX wall and because of the relative large CFHX volume (the flow channel is 50 μm high and 2 mm wide), this does not affect the mass flow. The partial pressure of water inside the nitrogen gas is reduced from 1 Pa at 200 K to about 10^{-10} Pa at 100 K which corresponds to a contamination of only about 10^{-11} ppm, in other words

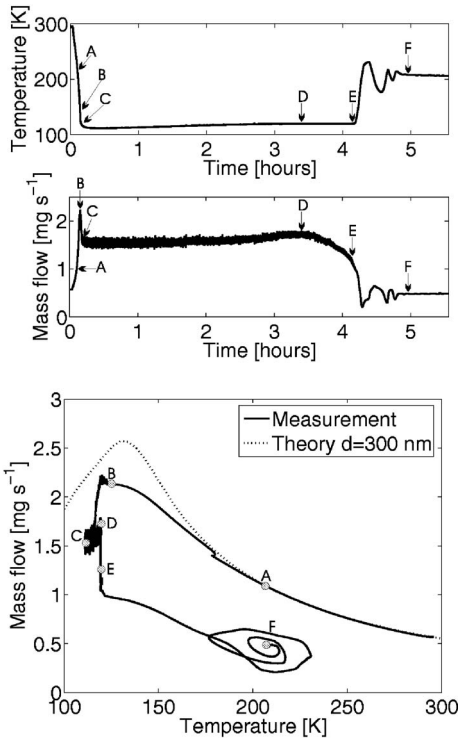

FIG. 2. Cooldown measurement of the cold stage.

nearly zero, see Fig. 1. A large portion of the water, about 99.9%, deposits in the CFHX area with a temperature between 200 and 160 K (main deposition area, see Fig. 1). From this point, the water contamination inside the nitrogen gas has decreased by a factor of 10^3 (i.e., from 1 to 10^{-3} Pa). From point C to D the temperature of the cold tip increases slightly because of condensation of residual air molecules in the vacuum space at the outside of the cooler. The surface of the cold stage is covered with a reflective gold layer of which the emissivity increases. During a long period of time (in this experiment 3 h from point C to D) nearly all water molecules deposit inside the main deposition area creating a thin layer of ice crystals on the CFHX surface. We assume that as this layer grows thicker, at some point the cohesion between the crystals becomes so weak that they disconnect and diffuse through the CFHX forced by the flow. When they reach the restriction, they get stuck inside and block the flow (point D to E). The mass flow decreases and as a result the cooling power drops. At a certain point (t=4.2 h, point E), the cooling power can no longer compensate for parasitic heat losses and the tip temperature increases. Due to this temperature increase, the mass flow decreases further and the cold tip heats up returning to a stable situation (F).

In a similar experiment, a cold stage was used without a gold layer on the outside so that it was possible to look inside the glass cooler during operation. Figure 3 shows four frames of a video that was taken during cooldown, showing the deposited water inside the cooler. In this experiment, as in the previous one, most of the water deposits in the main deposition area of the CFHX for a long period of time. As a result of the clogging of the restriction, the mass flow drops and the cold stage starts to warm up (point 1). In the corresponding frame no solid water can be seen in the filmed area. As the evaporator and the restriction warm up, the temperature gradient over the CFHX decreases and the main deposition area moves toward the cold tip. This is visualized in Fig. 3 by subtracting frame 1 from frame 2. At 2, the temperature of evaporator has increased to such an extent that this transition zone enters the restriction and the evaporator. The evaporator temperature rises further to point 3. Now a large amount of solid water has moved from the CFHX into the evaporator. The clogging of the restriction has now reached a maximum (flow is minimum). A cloud of deposited water can now be seen in the movie frame. From 4 to 5, the evaporator reaches the sublimation temperature and the

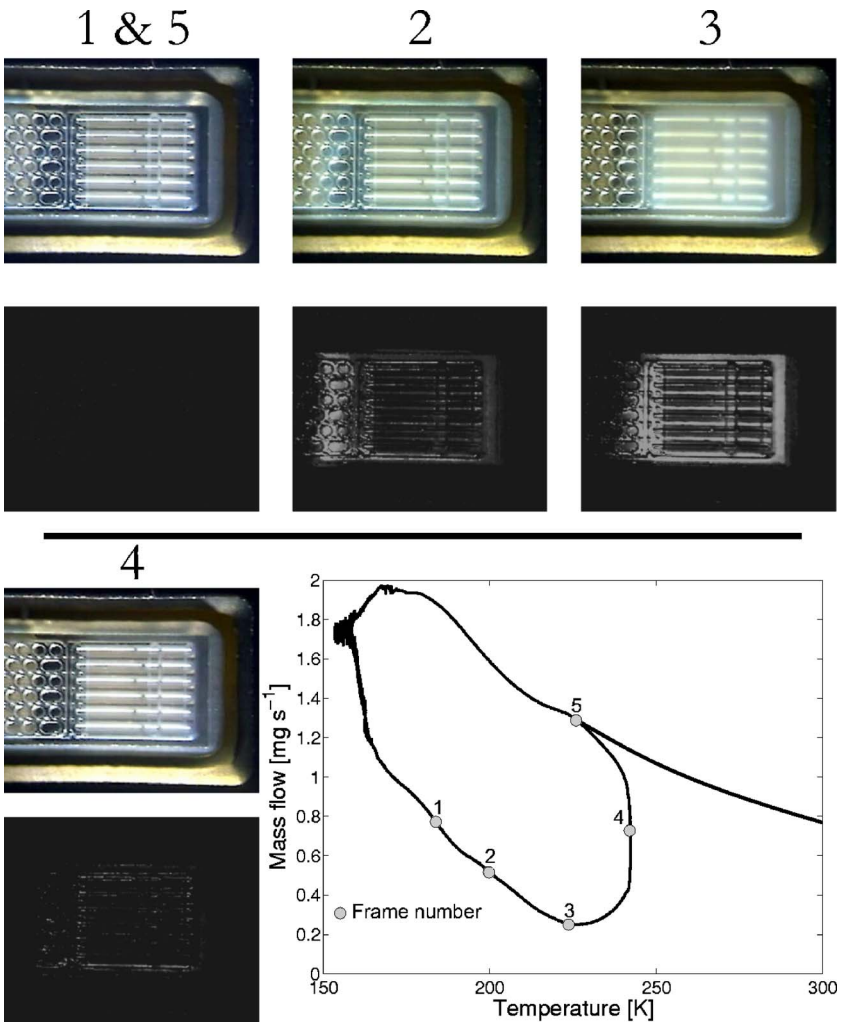

FIG. 3. Six different frames of a movie taken from the tip of the cold stage during operation. Below every frame a subtraction of the current frame and frame 1 is depicted. Bottom right: measurement data.

deposited water transitions back to vapor and is dragged away with the flow. The system now contains no more solid water molecules and the mass flow has returned to its original value so the cold stage can cool down again (point 5, the corresponding frame is the same as for 1). In contrast to the measurement shown in Fig. 2, a stable end situation is not reached. This is because there is no reflective shield on the evaporator, increasing the local parasitic heat loss and therefore the temperature lies above the local sublimation temperature of water.

In summary, the clogging of MEMS based microcoolers was investigated. Water molecules deposit inside the CFHX and deposited ice crystals migrate to the flow restriction, thus blocking the flow and reducing the cooling power. As a result, the cold tip warms up and the water deposition area moves to the evaporator part. A video taken during cooldown shows the deposited water inside the cooler that sublimates back to vapor, thus declogging the system. In the future, these microcoolers will be combined with small compressors, thus establishing closed-cycle microrefrigerators. By carefully pumping and purging these devices prior to closing, the amount of residual water can be limited. The remaining water will be trapped in the CFHX and can be sublimated back to vapor as described above. A small heater at the cold tip can be applied to force this process. We anticipate that in a few steps all water present in the system can be moved through the cold stage and collected at the warm end by adequate filtering. In this respect, the application of sorption compressors is very attractive.[11,12]

This work is supported by the Dutch Technology Foundation (STW) under Project No. TTF.5677.

[1]C. C. Yang, B. L. Nelson, B. R. Allen, W. L. Jones, and J. B. Horton, IEEE Trans. Microwave Theory Tech. **41**, 992 (1993).
[2]A. Mahdi and D. Mapps, Sens. Actuators, A **81**, 367 (2000).
[3]P. P. P. M. Lerou, G. Venhorst, C. Berends, T. T. Veenstra, M. Blom, J. F. Burger, H. J. M. ter Brake, and H. Rogalla, J. Micromech. Microeng. **16**, 1919 (2006).
[4]S. Garvey, S. Logan, R. Rowe, and W. A. Little, Appl. Phys. Lett. **42**, 1048 (1983).
[5]S. Jeong, Int. J. Refrig. **27**, 309 (2004).
[6]P. P. P. M. Lerou, T. T. Veenstra, J. F. Burger, H. J. M. ter Brake, and H. Rogalla, Cryogenics **45**, 659 (2005).
[7]H. Henmi, S. Shoji, Y. Shoji, K. Yoshimi, and M. Esashi, Sens. Actuators, A **43**, 243 (1994).
[8]Y.-T. Cheng and W.-T. Hsu, J. Microelectromech. Syst. **11**, 556 (2002).
[9]B. Lee, S. Seok, and K. Chun, J. Micromech. Microeng. **13**, 663 (2003).
[10]A. Roth, *Vacuum Technology*, 3rd ed. (Elsevier, Amsterdam, 1990), pp. 123–148.
[11]J. F. Burger, H. J. M. ter Brake, H. Rogalla, and M. Linder, Cryogenics **42**, 97 (2002).
[12]G. Wiegerinck, J. Burger, H. Holland, E. Hondebrink, H. J. M. ter Brake, and H. Rogalla, Cryogenics **46**, 9 (2006).
[13]Cryodata Inc. (http://www.cryodata.com).